

1
2 **Antarctic Sea Ice Prediction with A Convolutional Long Short-Term Memory**
3 **Network**

4 **Xiaoran Dong¹, Yafei Nie¹, Qinghua Yang^{1*}, Lorenzo Zampieri², Jiuke Wang³, Jiping Liu¹,**
5 **Dake Chen¹**

6 ¹School of Atmospheric Sciences, Sun Yat-sen University, and Southern Marine Science and
7 Engineering Guangdong Laboratory (Zhuhai), 519082 Zhuhai, China.

8 ²Ocean Modeling and Data Assimilation Division, Fondazione Centro Euro-Mediterraneo sui
9 Cambiamenti Climatici - CMCC, Bologna, Italy.

10 ³School of Artificial Intelligence, Sun Yat-sen University, 519082 Zhuhai, China.

11
12 Corresponding author: Qinghua Yang (yangqh25@mail.sysu.edu.cn)

13
14 **Key Points:**

- 15 • A convolutional long short-term memory (ConvLSTM) network is constructed to predict
16 the Antarctic sea ice for the next 60 days
- 17 • The ConvLSTM network exhibited predictive skill of about 1 month in predicting daily
18 spatial patterns of the Antarctic Sea ice concentration
- 19 • The ConvLSTM network can predict the sea ice extent maximum and minimum 1 month
20 in advance
21

22 **Abstract**

23 Antarctic sea ice predictions are becoming increasingly important both scientifically and
24 operationally due to climate change and increased human activities in the region. Conventional
25 numerical models typically require extensive computational resources and exhibit limited
26 predictive skill on the subseasonal-to-seasonal scale. In this study, a convolutional long short-term
27 memory (ConvLSTM) deep neural network is constructed to predict the 60-day future Antarctic
28 sea ice evolution using only satellite-derived sea ice concentration (SIC) from 1989 to 2016. The
29 network is skillful for approximately one month in predicting the daily spatial distribution of
30 Antarctic SIC between 2018 and 2022, with the best prediction skill found from June to September.
31 ConvLSTM can also successfully predict extreme Antarctic sea ice extent (SIE) one month in
32 advance, with the monthly mean SIE error mostly below 0.2 million km², suggesting substantial
33 potential for the application of machine learning techniques for skillful Antarctic sea ice prediction.

34 **Plain Language Summary**

35 Predicting the Antarctic sea ice evolution tends to be difficult due to the complex interaction
36 between the components of the climate system in the polar regions. Here we introduce a
37 convolutional long short-term memory (ConvLSTM) deep neural network, which is capable of
38 representing the non-linear relationships between the predictors and predictands to formulate
39 actual predictions on the evolution of the Antarctic sea ice cover up to 60 days in the future. Such
40 machine learning-based approaches are emerging as alternatives to traditional prediction systems,
41 where the prediction is informed by fundamental physical principles and empirical
42 parameterizations. Our retrospective forecast experiments reveal that the ConvLSTM exhibits
43 predictive skill of about one month in predicting daily spatial patterns of the Antarctic SIC between
44 2018 and 2022, and yields satisfactory performances in capturing unusually low sea ice conditions.
45 These encouraging results show the great potential of machine learning applications in the field of
46 Antarctic sea ice prediction.

47 **1 Introduction**

48 Antarctic sea ice is a crucial component of the climate system. Its seasonal variability has a
49 regulatory effect on the salinity structure of the Southern Ocean (Haumann et al., 2016; Goosse et
50 al., 2018), CO₂ uptake and release (Delille et al., 2014; Gray et al., 2018), and the global ocean
51 circulation (e.g., Pellichero et al., 2018). In recent years, with increased human activities (e.g.,
52 fishing, scientific research, tourism and associated logistics), skillful subseasonal-to-seasonal (S2S)
53 predictions of the Antarctic sea ice are becoming important to ensure safety and efficiency for
54 these operations (Jung et al., 2016; Tejedo et al., 2022; Liu et al., 2022). Motivated by these
55 scientific and practical necessities, the investigation of S2S prediction skill and predictability
56 increasingly became a priority of the scientific community (Holland et al., 2013; Alley et al., 2019;
57 Steele et al., 2021) and community projects, such as the Sea Ice Prediction Network South (SIPN
58 South) (Massonnet et al., 2023), have emerged.

59 Sea ice prediction, in particular on the S2S time scale, has traditionally been a challenge for polar
60 researchers (e.g., Jung et al., 2016; Guemas et al., 2016; Zampieri et al., 2018; Zampieri et al.,
61 2019; Xiu et al., 2022). To date, coupled numerical models are the main tool for S2S sea ice
62 forecasting in polar regions (Holmes et al., 2022), and the output of these models is distributed,
63 for example, by the Copernicus Climate Change Service (C3S) (<https://climate.copernicus.eu/>) or
64 the World Weather Research Program and the World Climate Research Program

65 (WWRP/WCRP) S2S Project (<http://www.s2sprediction.net>). Although S2S Antarctic sea ice
66 predictions are believed to have promising potential and skillful winter sea ice extent (SIE)
67 predictions up to 11 months in advance have been achieved in some regions (Bushuk et al., 2021),
68 only one model currently has the predictive skill in terms of sea ice edge better than a
69 climatological prediction at a lead time of 30 days (Zampieri et al., 2019). Improving Antarctic
70 sea ice forecasting with coupled models still requires substantial effort for better parameterizations,
71 initialization, increased spatial resolution, etc. An alternative but valuable method is formulating
72 sea ice prediction based on statistical models, which exploits recurrent predictor-predictand
73 relationships in past data (e.g., Chen and Yuan, 2004; Wang et al., 2016; Pei, 2021). For the
74 Antarctic SIE, statistical models exhibit better performance than dynamical models in practical
75 prediction exercises (Massonnet et al., 2023). However, the predictive skill of these statistical
76 models is largely constrained by their insufficient nonlinear fitting capability (Wang et al., 2013).
77 Given the abovementioned limitations of climate and statistical models, there is an urgent need for
78 a more efficient strategy to deal with the highly-nonlinear problem of S2S Antarctic sea ice
79 prediction.

80 Deep Learning (DL) is a technique in the field of artificial intelligence (AI) that uses a deep neural
81 network (DNN) to well capture the highly-nonlinear relationship between the features (i.e.,
82 predictors) and labels (i.e., predictands) (Schmidhuber, 2015). In recent years, DL has been applied
83 to the sea ice prediction. Chi and Kim (2017) made the first attempt at using DL in the prediction
84 of Arctic sea ice based on a fully-connected neural network and a long short-term memory (LSTM)
85 network. Liu et al. (2021) predicted the weekly Arctic sea ice concentration (SIC) using a
86 convolutional LSTM (ConvLSTM), which has predictive skills of up to 6 lead weeks in the
87 operational forecast. Andersson et al. (2021) used an ensemble of U-Net to predict the binary sea
88 ice probability for the next 6 months and showed that the U-Nets predict the sea ice edge position
89 better than the SEAS5 model (Johnson et al., 2019) in extreme events. Ren et al. (2022) optimized
90 the structure of the U-Net, and their DNN is skillful in predicting the daily Arctic SIC up to 28
91 days in the future. However, most of the attempts at integrating AI and sea ice prediction are still
92 in their infancy. The DNNs still have limited skill in quantitative daily sea ice prediction, and a
93 coherent two-dimensional model for the prediction of the whole polar domain, rather than a time
94 series for each pixel or part of the region is strongly required. Kim et al. (2020) and Asadi et al.
95 (2021) trained 12 individual monthly models respectively for 12 calendar months. However, in
96 practical application, it is desirable to use a single model to consistently complete a task.
97 Importantly, as often happens in sea ice research, the existing literature is strongly focused on the
98 Arctic, while the application of machine learning (ML) techniques for the prediction of Antarctic
99 sea ice is less common.

100 This paper aims to construct and test a ConvLSTM DNN to predict daily Antarctic sea ice
101 concentration fields. ConvLSTM (Shi et al., 2015) is a neural network designed to deal with spatial
102 and temporal information simultaneously and thus should have the ability to capture the spatial
103 and temporal variation of sea ice. The scientific questions that we address in this study are the
104 following:

105 1) Can we perform reasonable sea ice concentration predictions by relying only on past SIC
106 observations?

107 2) How does the predictive skill of ConvLSTM vary regionally and seasonally?

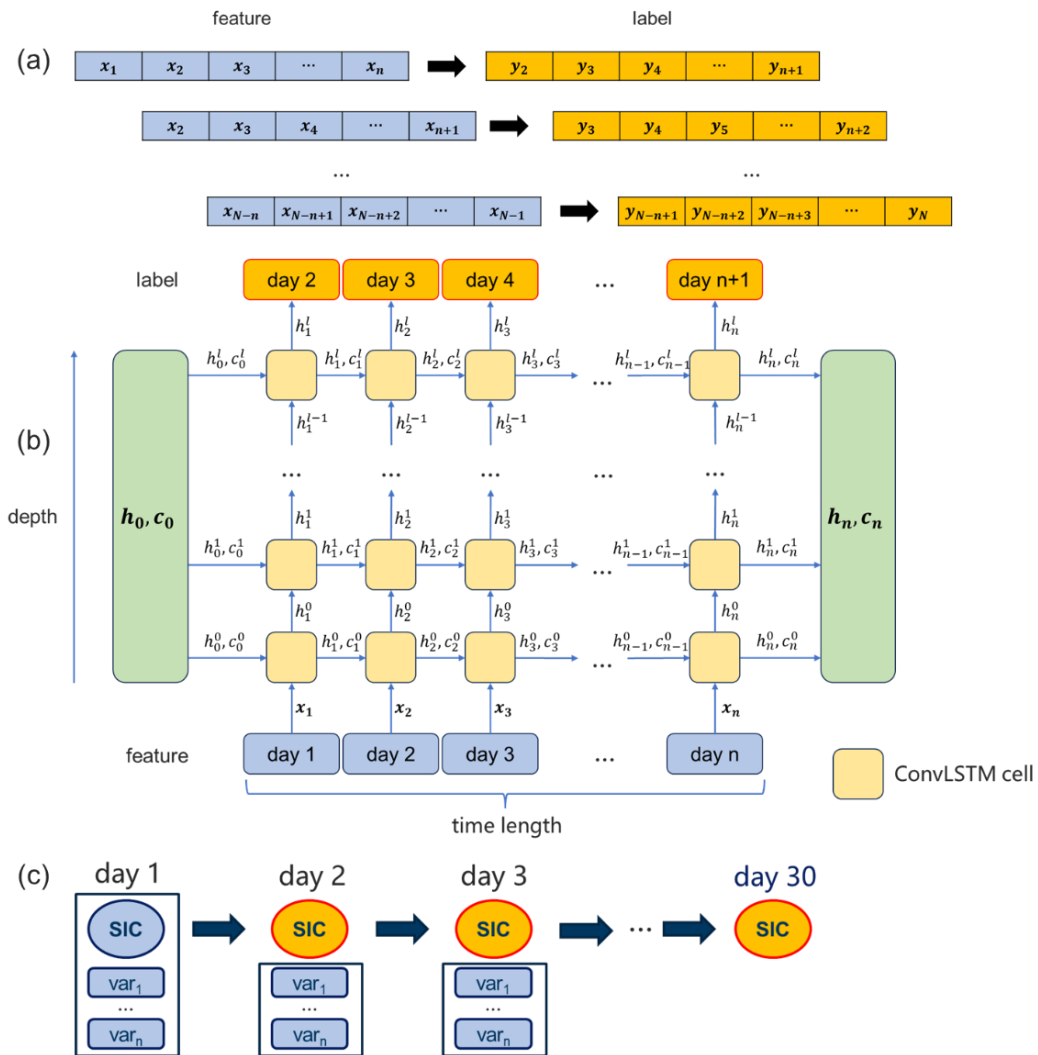
108 To the best of our knowledge, this is the first application of ConvLSTM in Antarctic sea ice
 109 prediction. Once ConvLSTM DNN is successfully constructed, it can also be easily employed to
 110 make predictions of the annual SIE, thus contributing to established initiatives of the sea ice
 111 prediction community, such as the SIPN-South project.

112 **2 Data and Methods**

113 **2.1 Model predictors and design of the training dataset**

114 The daily Antarctic sea ice concentration is the NASA-Team (Comiso, 2017), from 1st January
 115 1989 to 31st December 2021, released by the National Snow and Ice Data Center (NSIDC). In this
 116 paper, we regrid the SIC data from the original 25 km polar stereographic grid to the 100 km grid
 117 for the DL calculations. We divided the data into two groups. The data from January 1st, 1989 to
 118 December 31st, 2016 are assigned to the training set, and from January 1st, 2018 to December 31st,
 119 2022 to the independent testing set. The daily climatology and standard deviation of SIC are
 120 calculated from the training set.

121



122

123 **Figure 1.** Schematic diagram of ConvLSTM network for Antarctic sea ice concentration (SIC)
 124 prediction. (a) The feature-label dataset created with a rolling strategy. (b) The data flow of one
 125 sample in ConvLSTM. The inputs of day(1) – day(n) are regarded as features (i.e., the vector input
 126 into the model \mathbf{x}_i), and the outputs of day(2) – day(n+1) are regarded as labels. The \mathbf{h}_i represents
 127 the hidden variable, and the \mathbf{c}_i represents the cell state. (c) The schematic diagram for constrained
 128 prediction schemes. The variables within the blue area refer to the given data, and the variables
 129 within the orange area refer to the predicted data. The dark blue arrow signals that the model is
 130 calculated once forward in time.

131

132 In this study, we select six variables as the predictors. Three predictors are variables that contain
 133 SIC information: (1) the daily SIC data, (2) the daily climatology of SIC, and (3) its corresponding
 134 standard deviation. Three predictors are metadata or constant: the (4) sine and (5) cosine of the
 135 yearly time index, and (6) a gridded land mask (0 for land, 1 for ocean). It is worth noting that the
 136 metadata and constants employed here follow the approach of Andersson et al., 2021, such that
 137 the sine and cosine of the time index is a periodic sequence of 1 year. The dataset is created using
 138 a rolling strategy as illustrated in Figure 1a. \mathbf{x}_i represents the tensor containing six variables, and
 139 \mathbf{y}_i represents the SIC for prediction. In this way, more than 10000 samples are obtained from the
 140 training set. All variables except the metadata and constants are Gaussian-normalized before the
 141 input into the model.

142 2.2 The ConvLSTM neural network

143 ConvLSTM is a neural network that combines the CNN (Lecun et al., 1998) and LSTM
 144 (Hochreiter and Schmidhuber, 1997), by embedding the convolutional cells into LSTM cells (i.e.,
 145 ConvLSTM cell in Figure 1b). In this way, ConvLSTM can extract both spatial and temporal
 146 information and is a powerful tool for intricate 3D-spatiotemporal sequence prediction problems.
 147 Here we use a typical structure of the network and its hyperparameters: 5 hidden layers (the
 148 channel of which are [8,8,4,2,1]), kernel size of (5,5), a learning rate of 0.001, and weight decay
 149 of 0. The Mean Absolute Error (MAE) is used as the loss function, which is calculated for SICs
 150 across the entire Antarctic region between the ConvLSTM’s output and the corresponding SICs
 151 from the reanalysis. The ConvLSTM is trained with 300 epochs by applying a batch size of 32.
 152 The data flow of ConvLSTM of one sample is illustrated in Figure 1b. The time length of one
 153 sample is set to 90 days, thus the data of feature-label correspondence is a 90-day to 90-day series
 154 with a 1-day lag. Correspondingly, the constructed ConvLSTM model is a 1-lead prediction model.

155 In practical predictions, the model iterates the prediction result recurrently, with a self-constrained
 156 strategy (to be described in Sect. 2.3). We give the model the data from 90 days before the
 157 initialization date, including the initialization date, to initialize the model (i.e., the data from day[-
 158 89] to day[0]). The model will output the data for 90 days with a 1-day lag from the initialization
 159 (i.e., the predicted data is from day[-88] to day[1]). The last date (day[1]) is the predicted result
 160 for day[1] that we keep, while the first 89 days of prediction are discarded. Then, the data from
 161 day[-88] to day[1]—the features of day[1] are those just predicted—will be inputted into the model,
 162 and the model can output the predicted data of day[2]. Iteratively, we can get the predicted result
 163 for all the target days. The process of prediction can be summarized by Eq. 1:

$$164 \quad \text{label}_{pred[t_0+\delta t]} \\ 165 \quad = \text{ConvLSTM}(\text{feature}_{obs[t_0+\delta t-n, t_0+\delta t-n+1, \dots, t_0]} + \text{pred\&real}[t_0+1, t_0+2, \dots, t_0+\delta t-1])[-1] \quad (1)$$

166 where t_0 is the day of initialization, δt is the lead time, n is the time length (here 90 days), and
167 $[-1]$ means the last of the 90 outputs of ConvLSTM.

168 2.3 Self-constrained prediction strategy

169 Figure 1c shows the constrained prediction strategy. The constrained scheme is similar to Liu et
170 al. (2021), i.e., the real feature data are input into the model as features in long-time prediction. It
171 is a scheme that is usually used to test the maximum expected predictability given by the chosen
172 forecast methods and input fields. In this paper, the selected predictors are themselves information
173 on the sea ice, or alternatively metadata and constant. In this way, the predictors that are used to
174 constrain the predictands are known at the initialization, thus the model can make an operational
175 prediction using a constrained prediction strategy, which we call "self-constrained prediction
176 strategy".

177 3 Results

178 3.1 Predictive skill of ConvLSTM

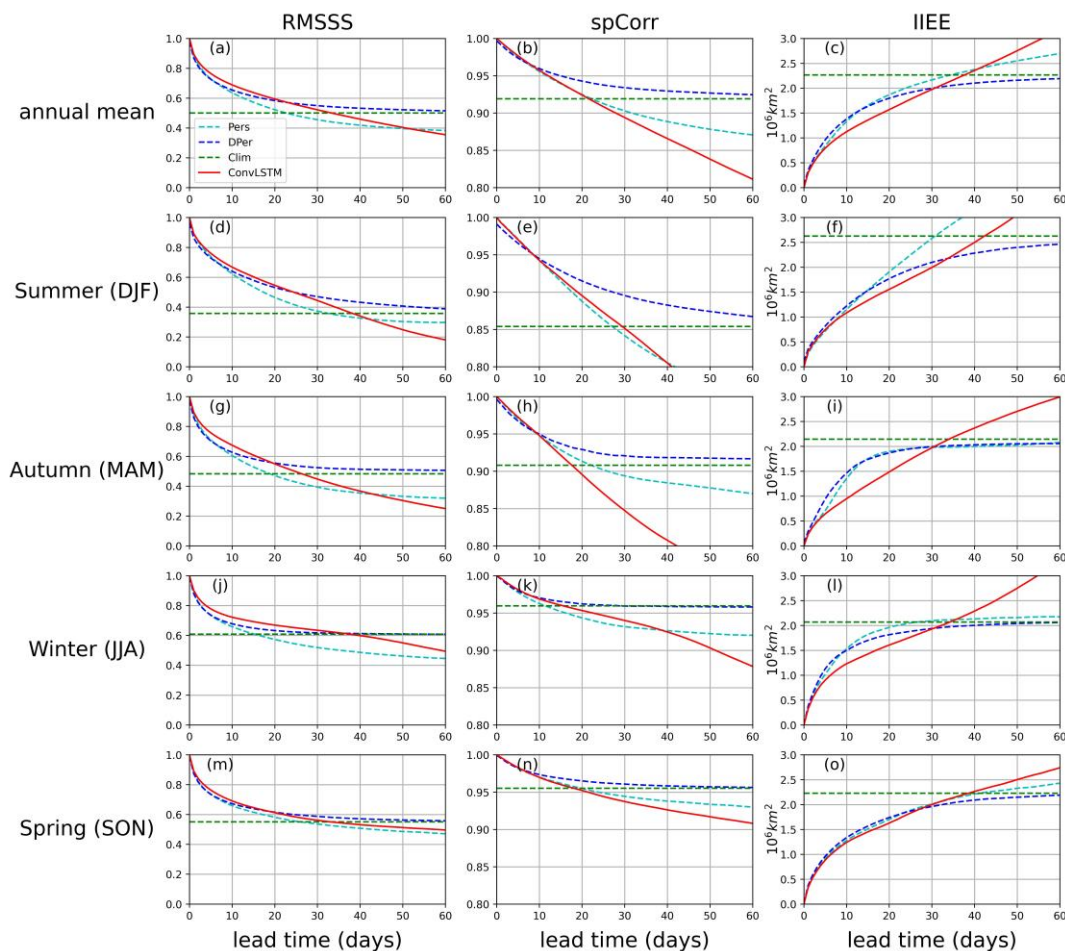
179 To assess the predictive skill, we use the Root-Mean-Square Skill Score (RMSSS, Barnston et al.,
180 2015), Spatial Correlation (spCorr), and Integrated Ice Edge Error (IIEE, Goessling, et al., 2016,
181 Goessling, 2018). Following Wang et al., (2018), we use three benchmark predictions, namely
182 climatology, anomaly persistence, and damped anomaly persistence, to further evaluate the
183 predictive skill of ConvLSTM. The skill metrics and benchmark predictions are described in detail
184 in the supporting information (Text S1). Figure 2 shows the hemispheric-averaged metrics of
185 ConvLSTM and the three benchmark predictions. Of the three benchmark predictions, the damped
186 anomaly persistence is the most skillful at short lead times, while the climatology is superior after
187 about 30 forecast days. Based on the climatological benchmark, the SIC prediction skill is best in
188 the austral winter (JJA) (Figures 2j to 2l), while it is worst in the summer (Figures 2d to 2f). When
189 compared to the damped anomaly persistence, the memory of spCorr is more skillful in terms of
190 the RMSSS and IIEE metrics, and its performance steadily approaches that of the two benchmark
191 forecasts as the lead time increases.

192 In terms of RMSSS metrics, ConvLSTM remains skillful for over 40 days compared to the
193 anomaly persistence throughout the year (the first column of Figure 2) and holds predictive skill
194 for 20 days compared to the damped anomaly persistence (Figure 2a). During the austral winter
195 and spring (SON), the ConvLSTM beats simple anomaly persistence for up to 60 lead days and
196 shows the highest skill in JJA, when ConvLSTM beats all three benchmarks up to 40 days. As
197 shown by the spCorr metric, the ConvLSTM-predicted SIC does not have a higher spatial
198 correlation with the observations compared to that of the (damped) anomaly persistence
199 benchmark, and this correlation decreases rapidly with time (Figure 2b). In austral summer (DJF)
200 and winter (JJA), the ConvLSTM shows only an overall skill of 20 days compared to the
201 climatological benchmark (Figure 2b) and a modest skill of 40 days compared to the anomaly
202 persistence (Figures 2e, 2k).

203 In contrast to the moderate performance on the point-to-point SIC comparison metrics (i.e.,
204 RMSSS and spCorr), the ConvLSTM shows better skill in predicting the Antarctic sea ice edge,
205 which is relevant information for potential forecast users. Specifically, ConvLSTM has better
206 predictive skills than the damped anomaly persistence up to 30 forecast days (Figure 2c), a signal
207 significant in all seasons except spring (Figures 2f, 2i, and 2o). From the above comparison,

208 although the ConvLSTM is relatively unskilled in providing detailed spatial information of sea ice
 209 within the pack ice compared to the persistence benchmark, it performs better in predicting the
 210 distribution of sea ice edge. This is a general characteristic of AI predictions: they may be skillful
 211 enough for binary problems (e.g., the presence or not of sea ice in a grid cell), but less meaningful
 212 when examining the spatial variations of a continuous field in detail.

213



214

215 **Figure 2.** 2018 to 2022 pan-Antarctic annual mean prediction skill quantified by RMSSS (a),
 216 spCorr (b), and the IIEE (c). (d-e-f), (g-h-i), (j-k-l), and (m-n-o) are the same as (a-b-c) but for
 217 December to February (DJF), March to May (MAM), June to August (JJA), and September to
 218 November (SON), respectively. RMSSS = Root-Mean-Square Skill Score; spCorr = Spatial
 219 Correlation; IIEE = Integrated Ice Edge Error.

220

221 3.2 The spatial and temporal dependency of predictive skill of ConvLSTM

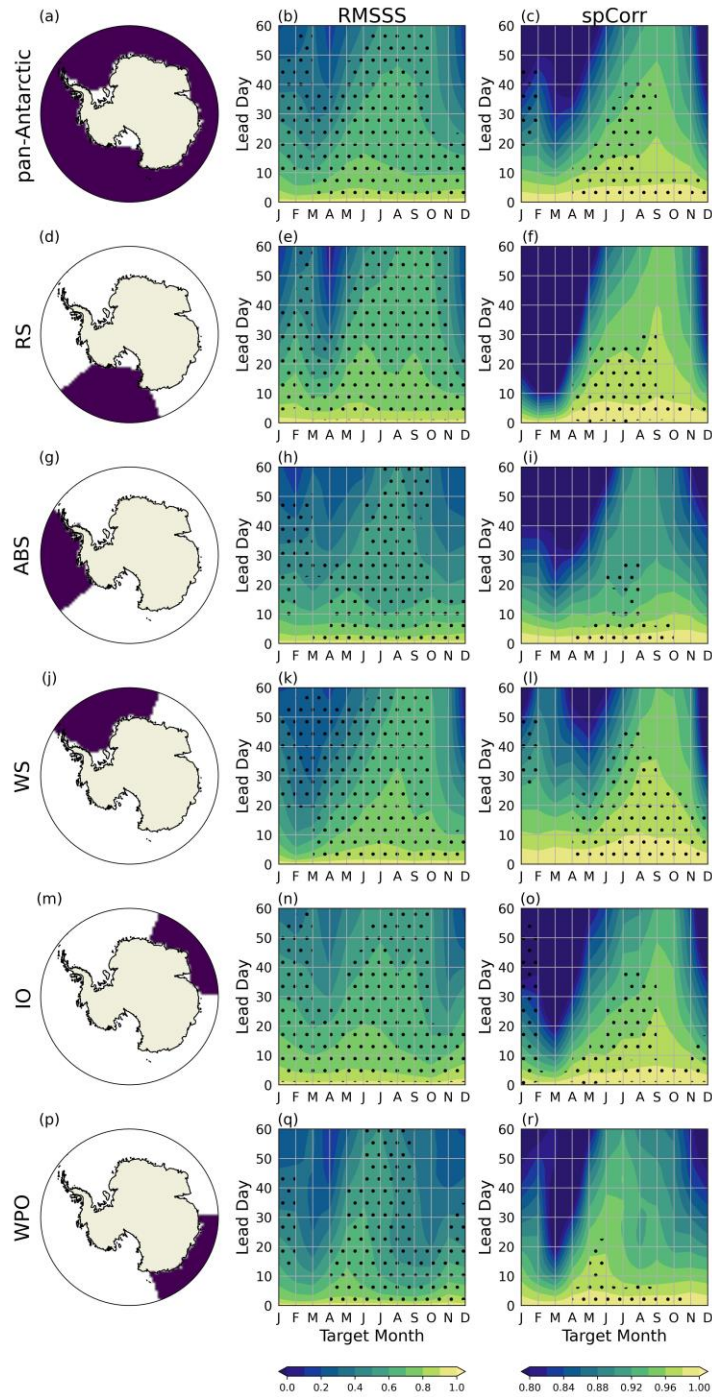
222 Since different sources of predictability characterize the sea ice in each sector of the Southern
 223 Ocean (Bushuk et al., 2021), the forecast predictive skill also significantly varies regionally and
 224 temporally (Zampieri et al., 2019). In this section, we present the predictive skill of ConvLSTM
 225 in each sector of the Southern Ocean, namely: the Ross Sea (RS, 160° E – 130° W), the

226 Amundsen/Bellingshausen seas (ABS, 130–60° W), the Weddell Sea (WS, 60° W–20° E), the
227 Indian Ocean (IO, 20–90° E), and the Western Pacific Ocean (WPO, 90–160° E). Figure 3 shows
228 the RMSSS and spCorr for regional SIC predictions of ConvLSTM. The skills vary by region and
229 season. It is found that the regional SIC skill is comparable to or exceeds that of the anomaly
230 persistence (refer to dot markers in Figure 3). For some target months and some regions, the
231 predictive skill outperforms the anomaly persistence up to 60 lead days, indicating that
232 ConvLSTM successfully captured some aspects of the sea ice variability at the S2S timescale.

233 The forecast skill shows a strong seasonal dependency. In terms of RMSSS, although the skill of
234 ConvLSTM is similar in each season for one-week predictions, it is lower in the austral autumn
235 (MAM) than in other seasons at the S2S timescale. The skills show diagonal features in all regions
236 in MAM and JJA, which means that the predictive skill is low when initialized in the Austral
237 summer. The high skill that emerged at the pan-Antarctic scale from winter to early spring (JJAS),
238 with the RMSSS exceeding 0.6 for up to 1 forecast month, also holds in the Ross Sea (RS),
239 Weddell Sea (WS), and Indian Ocean sector (IO), where ConvLSTM still outperforms the damped
240 anomaly persistence (supporting information Figure S1). On the contrary, in summer and autumn,
241 ConvLSTM shows relatively low skill at the S2S timescale, especially in April in the RS and the
242 WPO. As for the February prediction at 1 lead month, ConvLSTM performs better than the
243 anomaly persistence in the RS and IO but shows lower skill than anomaly persistence in ABS, WS,
244 WPO, and pan-Antarctic.

245 The diagonal feature is still evident in the spCorr plots(the second column of Figure 2). Here, the
246 diagonal feature peaks around September, revealing that the ConvLSTM has the highest skill for
247 SIC spatial variation in this month. Similar to the RMSSS, the skill peaks in May in the WPO,
248 suggesting that the season of the highest skill in this region is different from the others. The spCorr
249 is evidently low in DJF and MAM when the SIE is low (corresponding to Figures 2e and 2h).

250



251

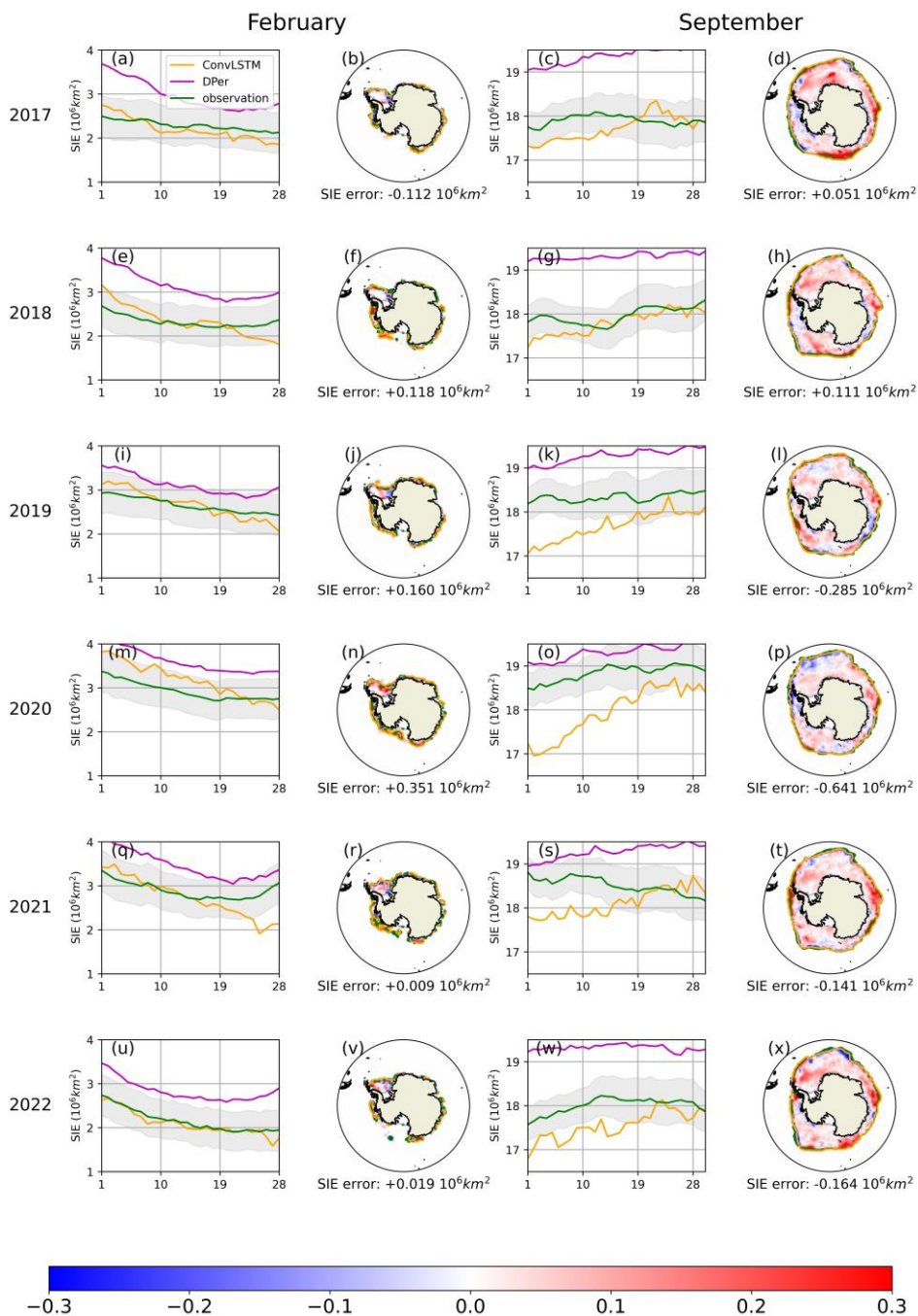
252 **Figure 3.** Seasonal predictive skill (RMSSS and spCorr) for the regional Antarctic SIC for
 253 different target months and prediction lead times. The six rows from top to bottom refer to pan-
 254 Antarctic, Ross Sea (RS), Amundsen and Bellingshausen Sea (ABS), Weddell Sea (WS), Indian
 255 Ocean (IO), and West Pacific Ocean (WPO), respectively. The dot markers indicate months where
 256 the skill of ConvLSTM beats the anomaly persistence forecast.

257

258 3.3 The prediction for February and September

259 To further examine the ConvLSTM's capability to predict the sea ice minimum and maximum, we
260 predict the SIE for February (sea ice minimum month) and September (sea ice maximum month)
261 from 2017 to 2022 at 1 month lead time. The results are shown in Figure 4. The ConvLSTM
262 generally gives a satisfactory prediction of the extent extremes. The difference between the
263 predicted and observed SIC is mostly below 20%. In February, the sea ice mainly concentrates in
264 the WS, and the prediction error in this sector varies by year. In February, ConvLSTM tends to
265 slightly overestimate the SIC in RS and WPO. In September, the SIC in the IO is overestimated
266 every year. However, the effects of overestimation and underestimation of SIC on the prediction
267 of sea ice edges are small, and the predicted position of the sea ice edge is in good agreement with
268 the observation (second and fourth columns of Figure 4).

269 In terms of the SIE (Figure 4), ConvLSTM's predictions are mostly in the range of one observed
270 standard deviation and generally more reliable than that of benchmark predictions (e.g., the
271 damped anomaly persistence). The SIE forecast error in September is generally larger than in
272 February and this could be explained by the annual variation of the sea ice edge length, which is
273 shorter in summer than in winter. It should be noted that in the February of 2017 and 2022, when
274 SIE hit record low values, the ConvLSTM made reliable predictions. The ConvLSTM prediction
275 shows a slight overestimation in February 2020 (Figure 4m) and an underestimation in September
276 2019 and 2020 (Figures 4k, 4o). The minimum SIE event of February 2022 is characterized by a
277 SIE decrease since September 2021 (Figure 4s), which the ConvLSTM fails to capture.



278

279 **Figure 4.** Comparison between the ConvLSTM 30-days predictions (orange lines), observations
 280 (green lines), and damped anomaly persistence (magenta lines) for February and September for
 281 the years 2017 to 2022. One standard deviation of the observations is displayed in gray shading.
 282 The maps show the difference between the predicted and observed monthly mean SIC in February
 283 2017, with the two ice edges indicated by the orange and green contours, respectively. The sea ice
 284 edge is the 15% contour of SIC.

285

286 **4 Summary and Outlook**

287 We constructed a ConvLSTM DNN model to predict the daily Antarctic SIC based solely on
288 information from the SIC observations. The model learns the information of one-step variation in
289 the training set from 1st January 1989 to 31st December 2016 and then is used for SIC reforecasting
290 from 2018 to 2022 through a self-constrained prediction strategy. By comparing the skills of the
291 ConvLSTM with three benchmarks, our results indicate that the ConvLSTM model can maintain
292 predictive skill for daily pan-Antarctic SIC for up to 1 lead month. The predictive skill of
293 ConvLSTM has significant seasonality, with better performance from June to September.
294 ConvLSTM also has good performances in predicting the SIE extremes 1 month in advance, with
295 monthly mean SIE error below 0.2 million km², and makes skillful predictions of the SIE record
296 low in 2017 and 2022.

297 Here, the design of the prediction method uses a self-constrained prediction strategy. Unlike the
298 sequence-to-sequence method, the length of the period of prediction can be changed flexibly,
299 which is preferred for practical applications of the prediction system. Indeed, operational
300 predictions can be achieved independently by using the data from the statistics of SIC, metadata,
301 and constant. As for the source of the predictive skill, we hypothesize that the SIC in the starting
302 day provides the model with the initialization state of SIC, and the region where the SIC is more
303 likely to change is provided by the standard deviation of SIC. The climatology, and sine/cosine of
304 time index provide the model with information on the day of the year and the potential tendency
305 of SIC. Finally, the land mask makes it possible for the model to distinguish between sea and land.
306 In this way, the model is expected to outperform both the (damped) anomaly persistence and
307 climatology prediction. The polar climate system is highly non-linear because of the ocean-ice-
308 atmosphere interactions. Thus, in the future, it might be necessary to introduce further oceanic or
309 atmospheric variables to improve the skills of ConvLSTM. For example, information on the
310 oceanic and atmospheric state could be provided from a dynamic numerical model, which would
311 require an evolution of the current self-constrained model to a constrained model that interacts
312 with a dynamical model.

313 Future work is still needed to improve the skills of the model. The ConvLSTM employed here is
314 based on a standard network structure, and it might benefit from customizations specific to the sea
315 ice prediction problem. The quality and uncertainty of data capability the capability of the model.
316 The amount of training samples is still small due to the limited observation record for SIC. This
317 could be improved by pre-training using extra data, for example from the Coupled Model
318 Intercomparison Project (CMIP, Eyring et al., 2016) database, which however provides only
319 limited skill for historic simulations of the Southern Ocean sea ice (Roach et al., 2020). Finally,
320 the computing power applied in this work is limited, and larger models could be tried in the future.

321 Nevertheless, this work reveals that by capturing only the sea ice statistics, without other oceanic
322 or atmospheric parameters, the DNN can formulate meaningful sea ice predictions and perform
323 better than typical benchmark predictions. Based on an analysis of the empirical orthogonal
324 functions for the sea ice concentration anomaly, which is included in the supplementary material
325 (Figure S2), we argue that this is not an easy task. According to this, the initial success of
326 ConvLSTM already shows that DNN can capture the tenuous non-linear relationships driving the
327 sea ice evolution in the Antarctic region. These encouraging results suggest the considerable
328 potential of applying this type of ML infrastructure to formulate reliable Antarctic sea ice
329 prediction.

330

331 **Acknowledgments**

332 This study is supported by the National Natural Science Foundation of China (No. 41941009),
 333 the National Key R&D Program of China (No. 2022YFE0106300), the Guangdong Basic and
 334 Applied Basic Research Foundation (No. 2020B1515020025), and the fundamental research
 335 funds for the Norges Forskningsråd (No. 328886). We acknowledge the National Snow & Ice
 336 Data Center (NSIDC) for producing and maintaining the sea ice concentration data. L.Z. was
 337 funded by the Foundation Euro-Mediterranean Center on Climate Change (CMCC, Italy).

338

339 **Conflict of Interest**

340 The authors declare no conflicts of interest relevant to this study.

341

342 **Data Availability Statement**

343 All data used here have open access. The daily sea ice concentration data are downloaded from
 344 National Snow & Ice Data Center, <https://nsidc.org/data/NSIDC-0051/versions/2>,
 345 <https://nsidc.org/data/NSIDC-0081/versions/2> (last access: May 2023). The network weights and
 346 design and the test dataset can be acquired from <https://doi.org/10.5281/zenodo.8137291>.

347

348 **References**

349

- 350 Alley, R. B., Cuffey, K. M., & Zoet, L. K. (2019). Glacial erosion: status and outlook. *Annals of*
 351 *Glaciology*, *60*(80), 1–13. <https://doi.org/10.1017/aog.2019.38>
- 352 Andersson, T. R., Hosking, J. S., Pérez-Ortiz, M., Paige, B., Elliott, A., Russell, C., et al. (2021).
 353 Seasonal Arctic sea ice forecasting with probabilistic deep learning. *Nature Communications*,
 354 *12*(1), 5124. <https://doi.org/10.1038/s41467-021-25257-4>
- 355 Asadi, N., Lamontagne, P., King, M., Richard, M., & Scott, K. A. (2022). Probabilistic
 356 spatiotemporal seasonal sea ice presence forecasting using sequence-to-sequence learning
 357 and ERA5 data in the Hudson Bay region. *The Cryosphere*, *16*(9), 3753–3773.
 358 <https://doi.org/10.5194/tc-16-3753-2022>
- 359 Barnston, A. G., Tippett, M. K., Van Den Dool, H. M., & Unger, D. A. (2015). Toward an improved
 360 multimodel ENSO prediction. *Journal of Applied Meteorology and Climatology*, *54*(7),
 361 1579–1595. <https://doi.org/10.1175/JAMC-D-14-0188.1>
- 362 Bushuk, M., Winton, M., Haumann, F. A., Delworth, T., Lu, F., Zhang, Y., et al. (2021). Seasonal
 363 prediction and predictability of regional Antarctic sea ice. *Journal of Climate*, 1–68.
 364 <https://doi.org/10.1175/JCLI-D-20-0965.1>
- 365 Chen, D., & Yuan, X. (2004). A Markov model for seasonal forecast of Antarctic sea ice. *Journal*
 366 *of Climate*, *17*(16), 3156–3168. [https://doi.org/10.1175/1520-0442\(2004\)017<3156:AMMFSF>2.0.CO;2](https://doi.org/10.1175/1520-0442(2004)017<3156:AMMFSF>2.0.CO;2)
- 368 Chi, J., & Kim, H. (2017). Prediction of Arctic sea ice concentration using a fully data driven Deep
 369 Neural Network. *Remote Sensing*, *9*(12), 1305. <https://doi.org/10.3390/rs9121305>
- 370 Comiso, J. C., Gersten, R. A., Stock, L. V., Turner, J., Perez, G. J., & Cho, K. (2017). Positive trend
 371 in the Antarctic sea ice cover and associated changes in surface temperature. *Journal of*
 372 *Climate*, *30*(6), 2251–2267. <https://doi.org/10.1175/JCLI-D-16-0408.1>
- 373 Delille, B., Vancoppenolle, M., Geilfus, N.-X., Tilbrook, B., Lannuzel, D., Schoemann, V., et al.
 374 (2014). Southern Ocean CO₂ sink: The contribution of the sea ice. *Journal of Geophysical*
 375 *Research: Oceans*, *119*(9), 6340–6355. <https://doi.org/10.1002/2014JC009941>

- 376 Eicken, H., Bhatt, U., Bieniek, P., Blanchard-Wrigglesworth, E., Wiggins, H., Turner-Bogren, B.,
377 et al. (2021). Moving sea ice prediction forward via community intercomparison. *Bulletin of*
378 *the American Meteorological Society*, 102(12), E2226–E2228.
379 <https://doi.org/10.1175/BAMS-D-21-0159.1>
- 380 Eyring, V., Bony, S., Meehl, G. A., Senior, C. A., Stevens, B., Stouffer, R. J., & Taylor, K. E. (2016).
381 Overview of the Coupled Model Intercomparison Project Phase 6 (CMIP6) experimental
382 design and organization. *Geoscientific Model Development*, 9(5), 1937–1958.
383 <https://doi.org/10.5194/gmd-9-1937-2016>
- 384 Goessling, H. F., & Jung, T. (2018). A probabilistic verification score for contours: Methodology
385 and application to Arctic ice-edge forecasts. *Quarterly Journal of the Royal Meteorological*
386 *Society*, 144(712), 735–743. <https://doi.org/10.1002/qj.3242>
- 387 Goessling, H. F., Tietsche, S., Day, J. J., Hawkins, E., & Jung, T. (2016). Predictability of the Arctic
388 sea ice edge. *Geophysical Research Letters*, 43(4), 1642–1650.
389 <https://doi.org/10.1002/2015GL067232>
- 390 Goosse, H., Kay, J. E., Armour, K. C., Bodas-Salcedo, A., Chepfer, H., Docquier, D., et al. (2018).
391 Quantifying climate feedbacks in polar regions. *Nature Communications*, 9(1), 1919.
392 <https://doi.org/10.1038/s41467-018-04173-0>
- 393 Gray, A. R., Johnson, K. S., Bushinsky, S. M., Riser, S. C., Russell, J. L., Talley, L. D., et al. (2018).
394 Autonomous biogeochemical floats detect significant carbon dioxide outgassing in the high-
395 latitude Southern Ocean. *Geophysical Research Letters*, 45(17), 9049–9057.
396 <https://doi.org/10.1029/2018GL078013>
- 397 Guemas, V., Blanchard-Wrigglesworth, E., Chevallier, M., Day, J. J., Déqué, M., Doblas-Reyes, F.
398 J., et al. (2016). A review on Arctic sea-ice predictability and prediction on seasonal to decadal
399 time-scales. *Quarterly Journal of the Royal Meteorological Society*, 142(695), 546–561.
400 <https://doi.org/10.1002/qj.2401>
- 401 Haumann, F. A., Gruber, N., Münnich, M., Frenger, I., & Kern, S. (2016). Sea-ice transport driving
402 Southern Ocean salinity and its recent trends. *Nature*, 537(7618), 89–92.
403 <https://doi.org/10.1038/nature19101>
- 404 Hochreiter, S., & Schmidhuber, J. (1997). Long short-term memory. *Neural Computation*, 9(8),
405 1735–1780. <https://doi.org/10.1162/neco.1997.9.8.1735>
- 406 Holland, M. M., Blanchard-Wrigglesworth, E., Kay, J., & Vavrus, S. (2013). Initial-value
407 predictability of Antarctic sea ice in the Community Climate System Model 3. *Geophysical*
408 *Research Letters*, 40(10), 2121–2124. <https://doi.org/10.1002/grl.50410>
- 409 Holmes, C. R., Bracegirdle, T. J., & Holland, P. R. (2022). Antarctic sea ice projections constrained
410 by historical ice cover and future global temperature change. *Geophysical Research Letters*,
411 49(10). <https://doi.org/10.1029/2021GL097413>
- 412 Johnson, S. J., Stockdale, T. N., Ferranti, L., Balsaseda, M. A., Molteni, F., Magnusson, L., et al.
413 (2019). SEAS5: the new ECMWF seasonal forecast system. *Geoscientific Model*
414 *Development*, 12(3), 1087–1117. <https://doi.org/10.5194/gmd-12-1087-2019>
- 415 Jung, T., Gordon, N. D., Bauer, P., Bromwich, D. H., Chevallier, M., Day, J. J., et al. (2016).
416 Advancing polar prediction capabilities on daily to seasonal time scales. *Bulletin of the*
417 *American Meteorological Society*, 97(9), 1631–1647. [https://doi.org/10.1175/BAMS-D-14-](https://doi.org/10.1175/BAMS-D-14-00246.1)
418 [00246.1](https://doi.org/10.1175/BAMS-D-14-00246.1)
- 419 Kim, Y. J., Kim, H.-C., Han, D., Lee, S., & Im, J. (2020). Prediction of monthly Arctic sea ice
420 concentrations using satellite and reanalysis data based on convolutional neural networks.
421 *The Cryosphere*, 14(3), 1083–1104. <https://doi.org/10.5194/tc-14-1083-2020>

- 422 Lecun, Y., Bottou, L., Bengio, Y., & Haffner, P. (1998). Gradient-based learning applied to
423 document recognition. *Proceedings of the IEEE*, 86(11), 2278–2324.
424 <https://doi.org/10.1109/5.726791>
- 425 Liu, H., Yu, W., & Chen, X. (2022). Melting Antarctic sea ice is yielding adverse effects on a short-
426 lived squid species in the Antarctic adjacent waters. *Frontiers in Marine Science*, 9, 819734.
427 <https://doi.org/10.3389/fmars.2022.819734>
- 428 Liu, Y., Bogaardt, L., Attema, J., & Hazeleger, W. (2021). Extended-range Arctic sea ice forecast
429 with convolutional long short-Term memory networks. *Monthly Weather Review*, 149.
430 <https://doi.org/10.1175/mwr-d-20-0113.1>
- 431 Massonnet, F., Barreira, S., Barthélemy, A., Bilbao, R., Blanchard-Wrigglesworth, E., Blockley,
432 E., et al. (2023). SIPN South: six years of coordinated seasonal Antarctic sea ice predictions.
433 *Frontiers in Marine Science*, 10, 1148899. <https://doi.org/10.3389/fmars.2023.1148899>
- 434 Merryfield, W. J., Lee, W.-S., Wang, W., Chen, M., & Kumar, A. (2013). Multi-system seasonal
435 predictions of Arctic sea ice. *Geophysical Research Letters*, 40(8), 1551–1556.
436 <https://doi.org/10.1002/grl.50317>
- 437 Pei, Y. (2021). Cyclostationary EOF modes of Antarctic sea ice and their application in prediction.
438 *Journal of Geophysical Research: Oceans*, 126(10). <https://doi.org/10.1029/2021JC017179>
- 439 Pellichero, V., Sallée, J.-B., Chapman, C. C., & Downes, S. M. (2018). The Southern Ocean
440 meridional overturning in the sea-ice sector is driven by freshwater fluxes. *Nature*
441 *Communications*, 9(1), 1789. <https://doi.org/10.1038/s41467-018-04101-2>
- 442 Ren, Y., Li, X., & Zhang, W. (2022). A data-driven deep learning model for weekly sea ice
443 concentration prediction of the pan-Arctic during the melting season. *IEEE Transactions on*
444 *Geoscience and Remote Sensing*, 60, 1–19. <https://doi.org/10.1109/TGRS.2022.3177600>
- 445 Roach, L. A., Dörr, J., Holmes, C. R., Massonnet, F., Blockley, E. W., Notz, D., et al. (2020).
446 Antarctic sea ice area in CMIP6. *Geophysical Research Letters*, 47(9).
447 <https://doi.org/10.1029/2019GL086729>
- 448 Schmidhuber, J. (2015). Deep learning in neural networks: An overview. *Neural Networks*, 61, 85–
449 117. <https://doi.org/10.1016/j.neunet.2014.09.003>
- 450 Shi, X., Chen, Z., Wang, H., Yeung, D.-Y., Wong, W., & WOO, W. (2015). Convolutional LSTM
451 network: A machine learning approach for precipitation nowcasting. In C. Cortes, N.
452 Lawrence, D. Lee, M. Sugiyama, & R. Garnett (Eds.), *Advances in Neural Information*
453 *Processing Systems* (Vol. 28). Curran Associates, Inc. Retrieved from
454 [https://proceedings.neurips.cc/paper_files/paper/2015/file/07563a3fe3bbe7e3ba84431ad9d0](https://proceedings.neurips.cc/paper_files/paper/2015/file/07563a3fe3bbe7e3ba84431ad9d055af-Paper.pdf)
455 [55af-Paper.pdf](https://proceedings.neurips.cc/paper_files/paper/2015/file/07563a3fe3bbe7e3ba84431ad9d055af-Paper.pdf)
- 456 Tejedo, P., Benayas, J., Cajiao, D., Leung, Y.-F., De Filippo, D., & Liggett, D. (2022). What are
457 the real environmental impacts of Antarctic tourism? Unveiling their importance through a
458 comprehensive meta-analysis. *Journal of Environmental Management*, 308, 114634.
459 <https://doi.org/10.1016/j.jenvman.2022.114634>
- 460 Wang, L., Yuan, X., Ting, M., & Li, C. (2016). Predicting summer Arctic sea ice concentration
461 intraseasonal variability using a vector autoregressive model. *Journal of Climate*, 29(4),
462 1529–1543. <https://doi.org/10.1175/JCLI-D-15-0313.1>
- 463 Wang, L., Yuan, X., & Li, C. (2019). Subseasonal forecast of Arctic sea ice concentration via
464 statistical approaches. *Climate Dynamics*, 52(7–8), 4953–4971.
465 <https://doi.org/10.1007/s00382-018-4426-6>
- 466 Xiu, Y., Luo, H., Yang, Q., Tietsche, S., Day, J., & Chen, D. (2022). The challenge of Arctic sea
467 ice thickness prediction by ECMWF on subseasonal time scales. *Geophysical Research*

- 468 *Letters*, 49(8). <https://doi.org/10.1029/2021GL097476>
469 Zampieri, L., Goessling, H. F., & Jung, T. (2018). Bright prospects for Arctic sea ice prediction on
470 subseasonal time scales. *Geophysical Research Letters*, 45(18), 9731–9738.
471 <https://doi.org/10.1029/2018GL079394>
472 Zampieri, L., Goessling, H. F., & Jung, T. (2019). Predictability of Antarctic sea ice edge on
473 subseasonal time scales. *Geophysical Research Letters*, 46(16), 9719–9727.
474 <https://doi.org/10.1029/2019GL084096>
475

476 **References From the Supporting Information**

- 477
478 Yuan, X., & Martinson, D. G. (2001). The Antarctic dipole and its predictability. *Geophysical*
479 *Research Letters*, 28(18), 3609–3612. <https://doi.org/10.1029/2001GL012969>
480